

# Mechanism of Low-Intermediate-High Confinement Transitions in HL-2A Tokamak

J.Q. Dong, J. Cheng, L.W. Yan, Z.X. He, K. Itoh, H. S. Xie, Y. Xiao,  
K. J. Zhao, W.Y. Hong, Z.H. Huang, L. Nie, S.-I. Itoh, W.L. Zhong,  
D.L. Yu , X.Q. Ji, Y. Huang, X.M. Song, Q.W. Yang, X.T. Ding,  
X.L. Zou, X. R. Duan, Yong Liu and HL-2A Team  
Southwestern Institute of Physics, Chengdu, China

*In collaboration with*

*Institute for Fusion Theory and Simulation, ZJU, Hangzhou,  
China*

*National Institute for Fusion Science, Toki, Japan*

*University of Science and Technology of China, Hefei, China*

*WCI Center for Fusion Theory, Daejeon, Korea*

*Kyushu University, Kasuga, Japan*

*CEA, IRFM, Cadarache, France*



# Outline

1. Introduction
2. Experimental setup
3. Experimental results
4. Summary and discussion



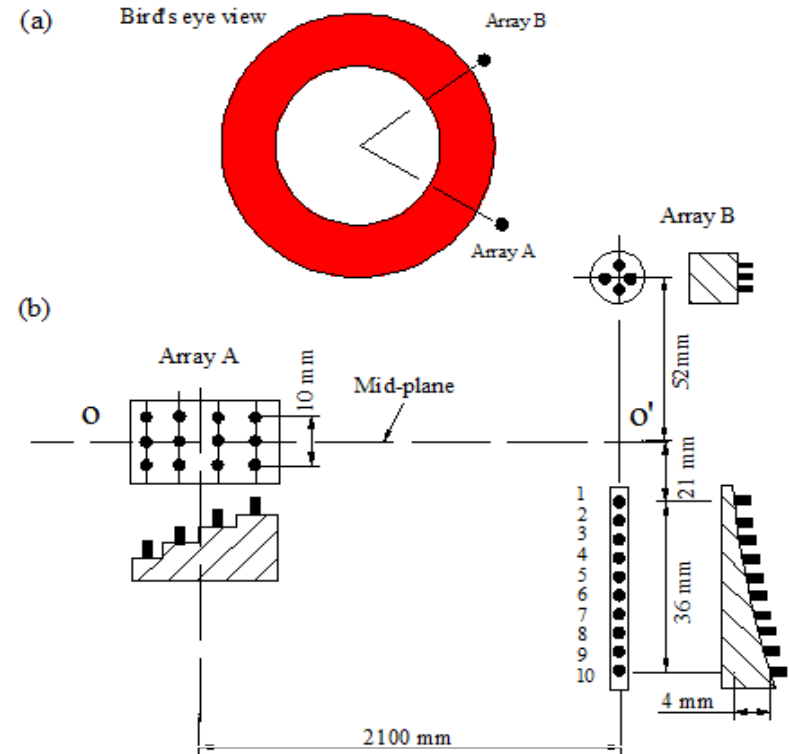
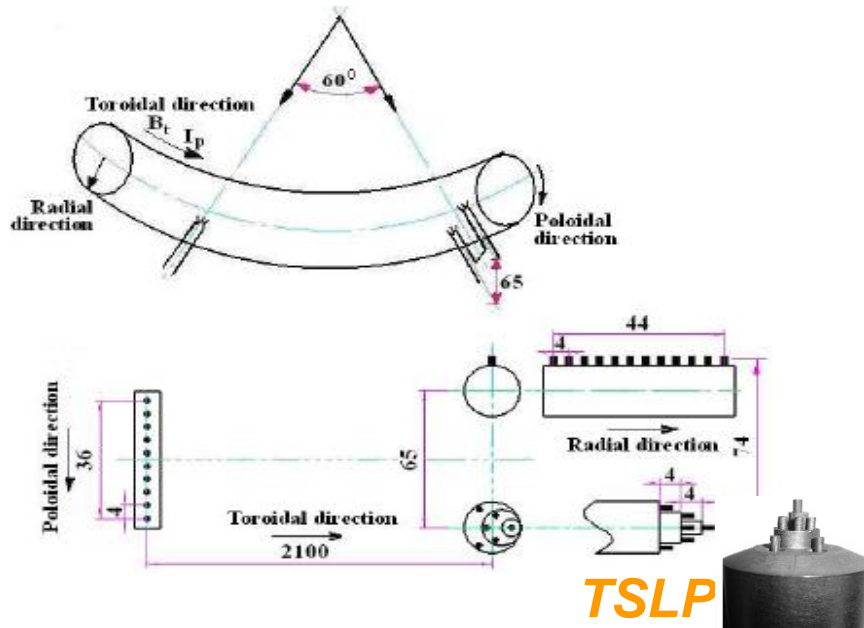
# 1. Introduction

- Identification of the key plasma parameters, which control/determine the L-H transition and reveal its mechanism, has been a long term focus of investigation and a topic of interest.
- Understanding of transition physics is essential for assessing power threshold scaling and ensuring heating power requirements for future fusion reactors such as ITER.
- Study on dynamics of limit cycle oscillations (LCOs) with expansion of time scale provides an opportunity to investigate the subject quantitatively.
- The LCOs have been studied theoretically with predator-prey and bifurcation models, respectively.
- In experiment, spontaneous LCOs were observed on JET, JFT-2M, AUG, DIII-D, EAST, NSTX, H-1, and TJ-II.
- Mechanism, trigger and onset conditions of the L-I-H transitions are investigated on HL-2A tokamak.



# 2. Experimental setup

## 3D Langmuir probe arrays



- Sampling rate = 1 MHz
- Spatial resolution = 3 mm
- Diameter of tips is 1.5 mm.
- Height of tips is 3 mm.

Parameters measured simultaneously:  
 $T_e, n_e, \phi_f, \tilde{n}_e, E_r, P_e, E'_r, P'_e$ ,  
 etc. at a few radial and poloidal positions in two poloidal sections;

Complete data of edge turbulence in tokamak plasmas.



# 3. Experimental results

## Shot I with L-I-H transitions

$B_t=1.4\text{ T}$ ,  $I_p=180\text{ kA}$

$P_{\text{NBI}}=1.0\text{ MW}$

$$\bar{n}_e = (2.8 - 3.2) \times 10^{19} \text{ m}^{-3}$$

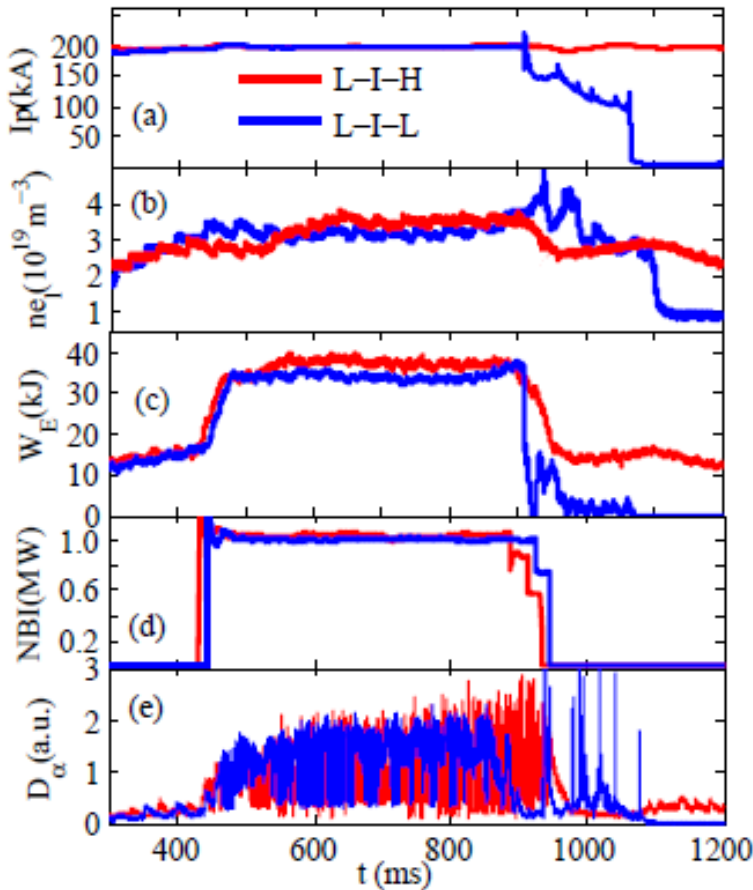
## Shot II with L-I-L transitions

$B_t=1.4\text{ T}$ ,  $I_p=185\text{ kA}$

$P_{\text{NBI}}=1.0\text{ MW}$

$$\bar{n}_e = (2.5 - 3.0) \times 10^{19} \text{ m}^{-3}$$

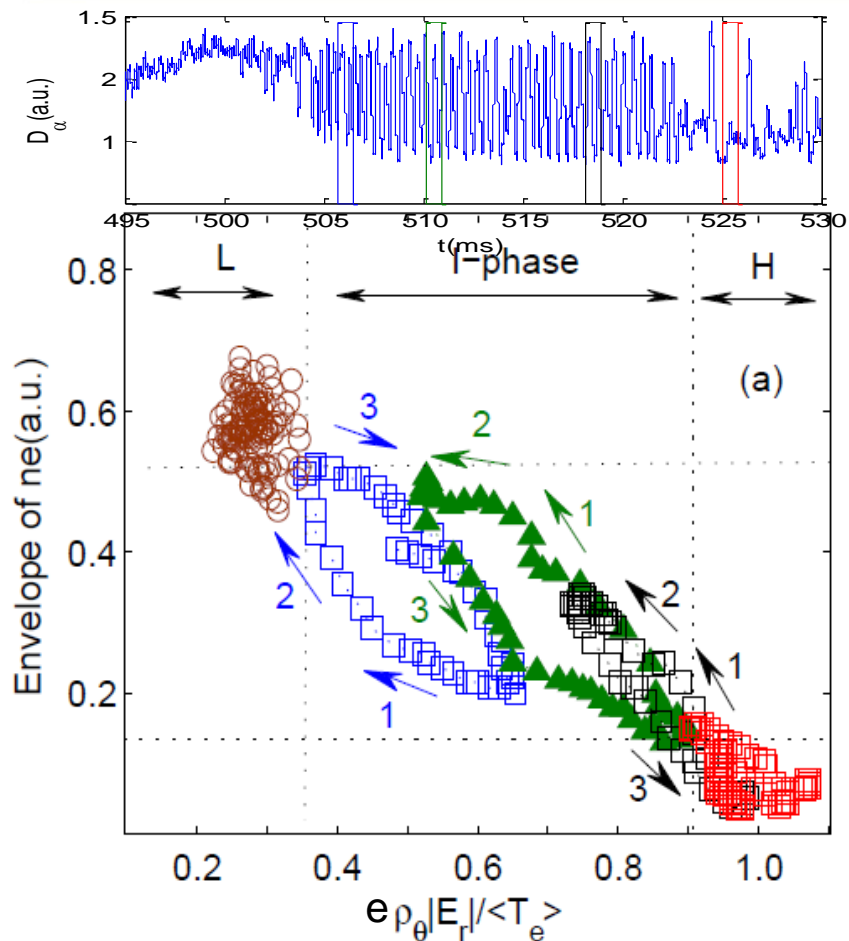
- Strong turbulent fluctuations of floating potentials and densities, and weak radial electric fields in the L-modes.
- Weak fluctuations of floating potentials and densities but strong radial electric fields in the I-phases.
- Rather weak fluctuations of floating potential and density but very strong radial electric field in the H-mode.



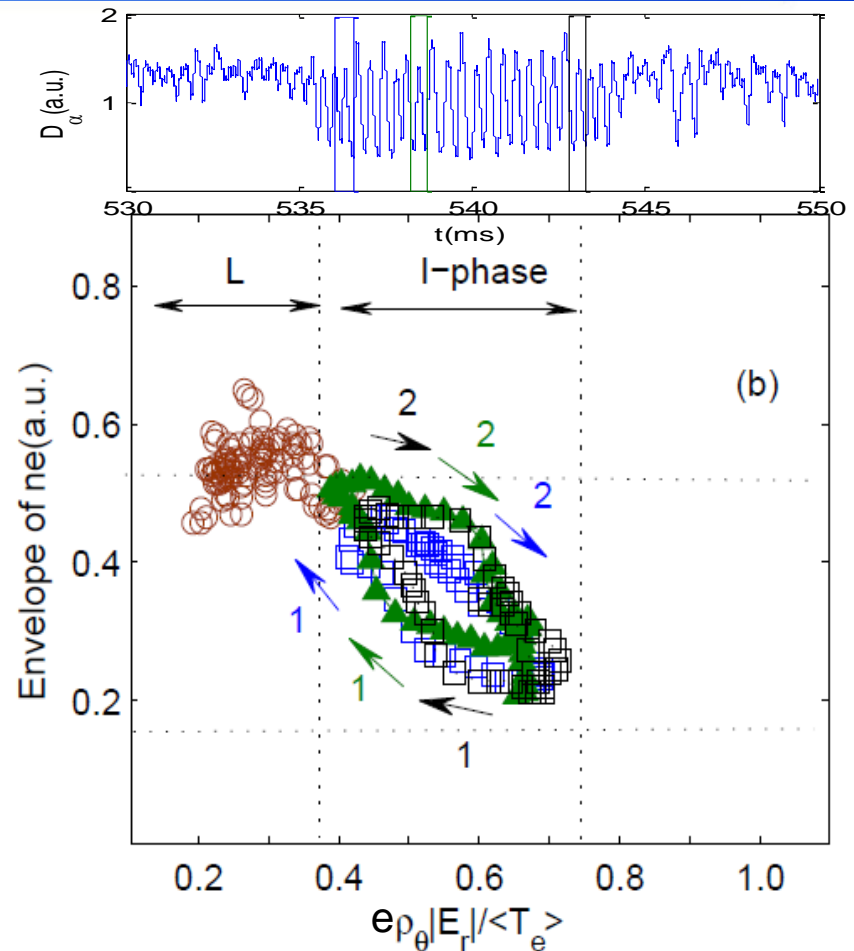
In the I-phases, all the fluctuations oscillate at same frequency of  $f_{\text{LCO}} \sim 2.6\text{ kHz}$  which is identified to be close to the local Ion-ion collision frequency.



# LCO in L-I-H & L-I-L transitions



$t=506-506.5$  ms,  $t=510-510.5$  ms,  
 $t=518-518.5$  ms,  $t=525-525.5$  ms.

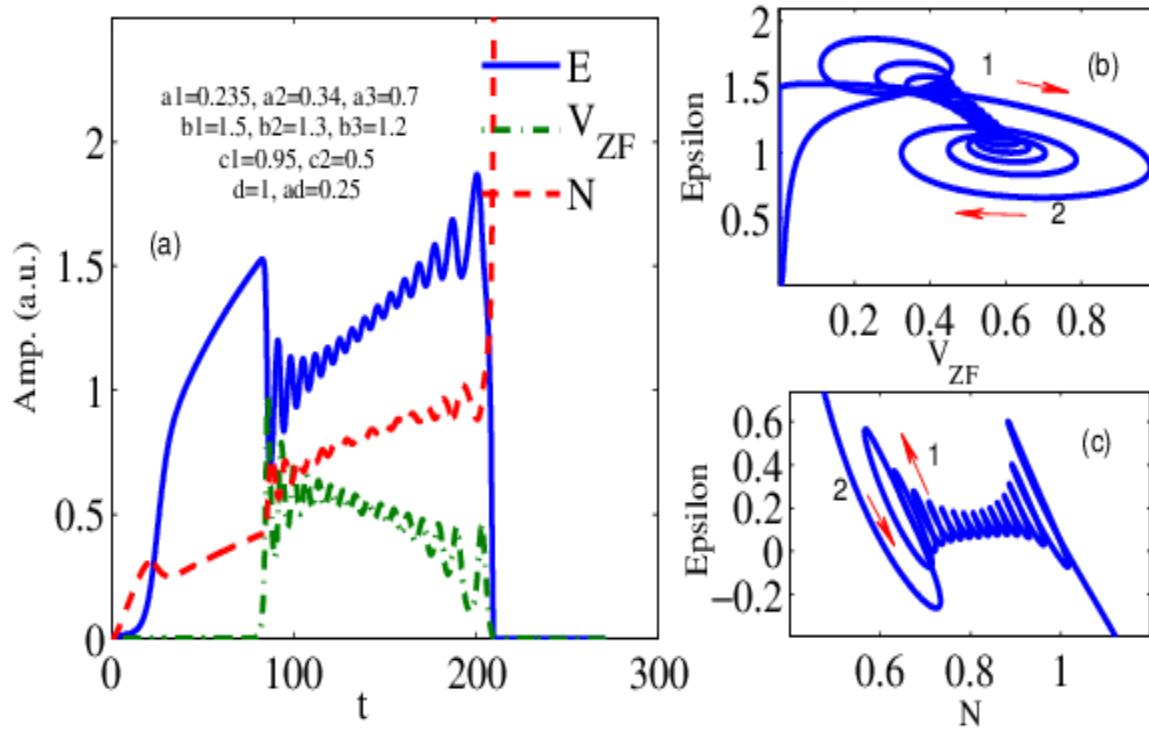


$t= 536-536.5$  ms,  $t=538.5-539$  ms,  
 $t=543-543.5$  ms.

[Cheng & Dong et al., PRL 110, 265002 (2013) ]



# Brief numerical analysis of LCOs



$$\frac{\partial \varepsilon}{\partial t} = N\varepsilon - a_1\varepsilon^2 - a_2V^2\varepsilon - a_3V_{zf}\varepsilon - a_dV\varepsilon,$$

$$\frac{\partial V_{zf}}{\partial t} = \frac{b_1\varepsilon V_{zf}}{1 + b_2V^2} - b_3V_{zf},$$

$$\frac{\partial N}{\partial t} = -c_1\varepsilon N - c_2N + Q,$$

$$V = dN^2.$$

**Kim, E.J. et al., 2003,  
PRL. 90185006.**

- (a)  $\varepsilon$ ,  $V_{zf}$  and  $N$  as functions of  $Q=0.01 t$ ,
- (b) the Lissajous diagram for  $\varepsilon$  vs.  $V_{zf}$  type-Y,
- (c) the Lissajous diagram for  $\varepsilon$  vs.  $N$  type-J,



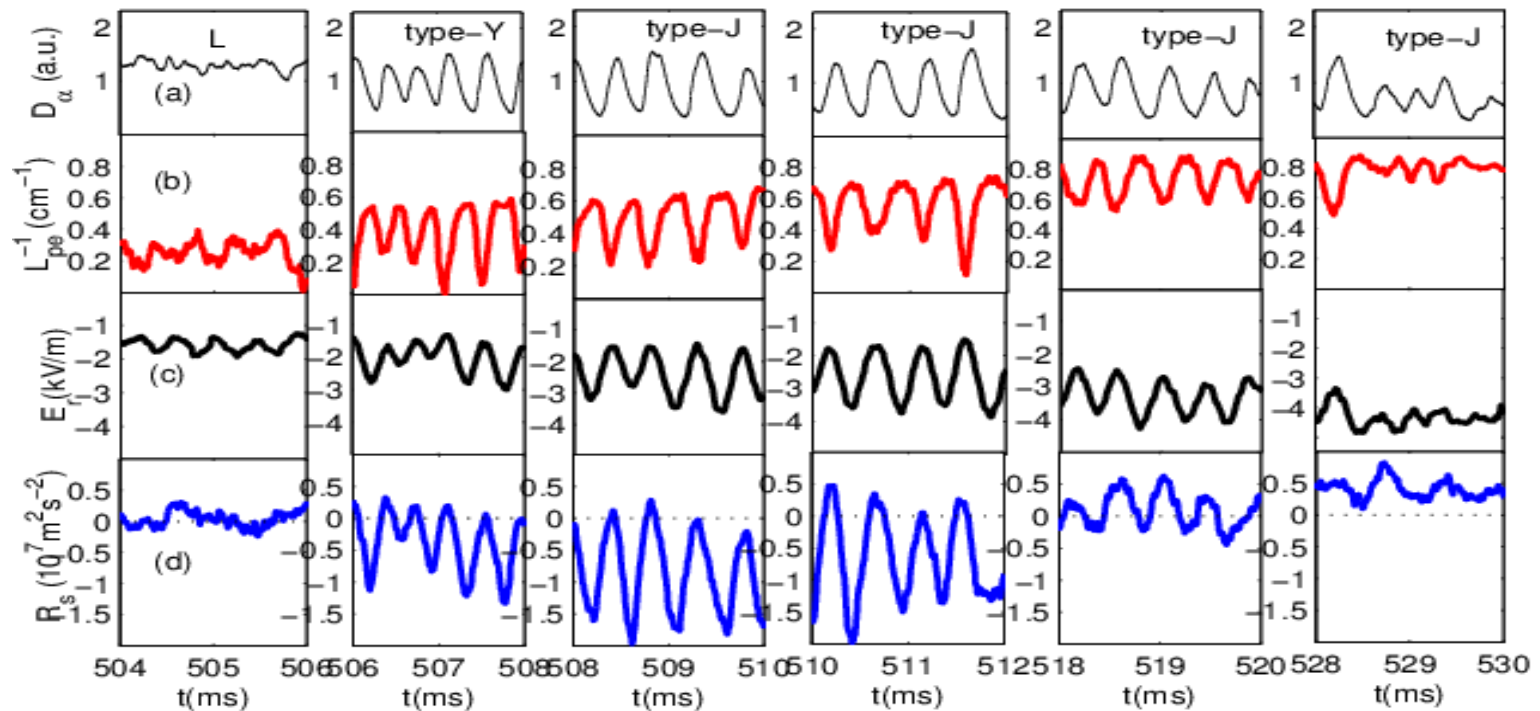
# Plausible loops for LCOs and I/L-H transition

Green for type-Y (CW) LCO,  
Red for type-J (CCW) LCO,  
yellow for I/L-H transition

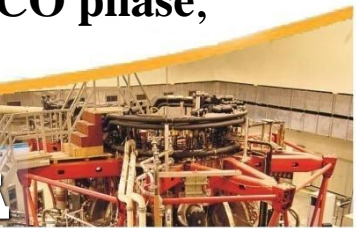




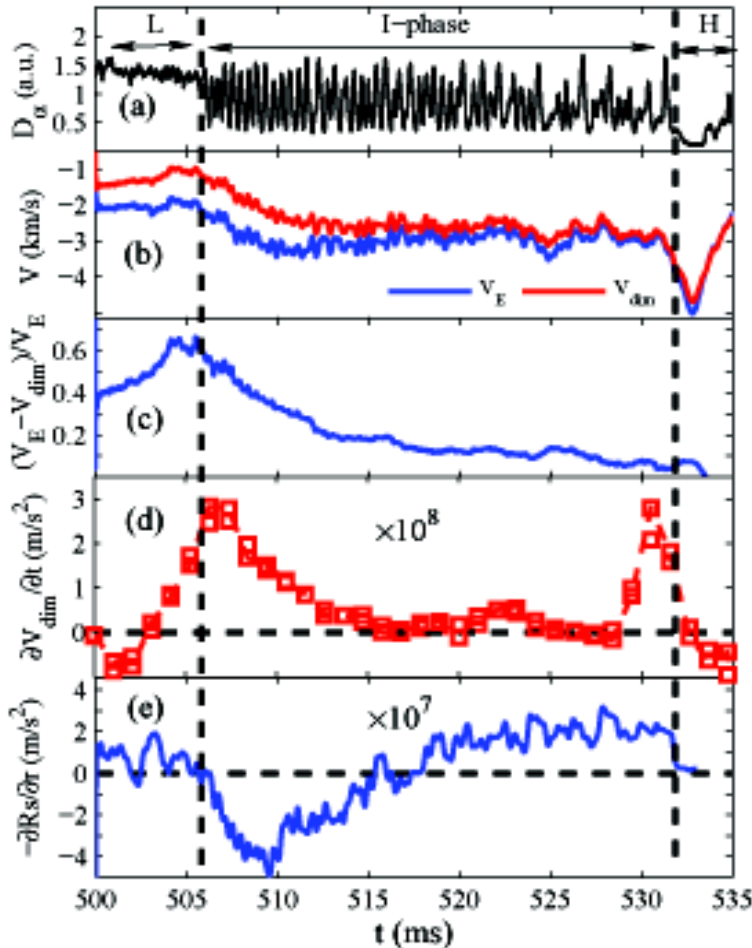
# LCOs of plasma parameters in L-I-H transitions



- The temporal evolutions of (a)  $D_\alpha$  emission, (b) inverse of the electron pressure gradient scale length  $1/L_{pe}$ , (c) the radial electric field  $E_r$ , and (d) the Reynolds stress  $R_s$ .
- $1/L_{pe}$  and  $|E_r|$  gradually increase; their oscillations are in phase
- $R_s$  is high/low and in/out of phase with  $|E_r|$  in early/late LCO phase,

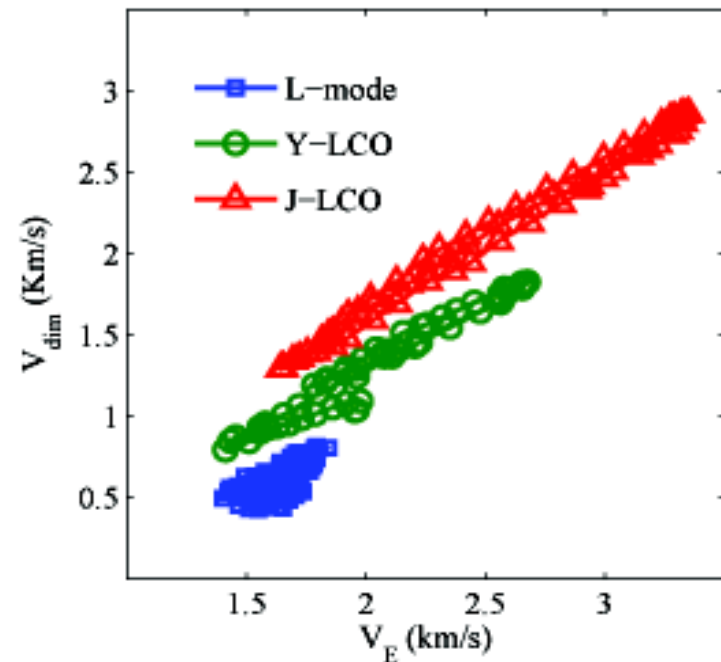


# $E \times B$ and diamagnetic flows averaged over LCOs



## Force balance equation of ions

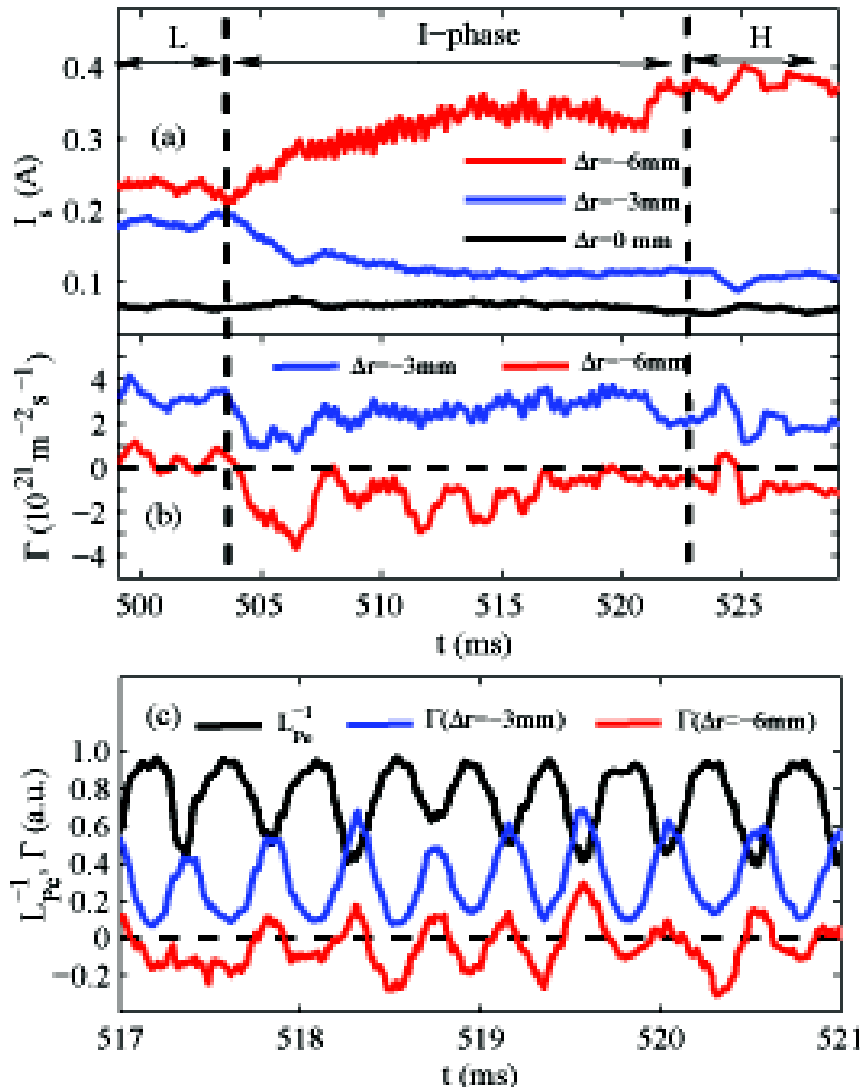
$$E_r = \underbrace{\frac{1}{n_i Z_i e} \nabla_r P_i(f)}_{E_{r, dim}} - \underbrace{v_{\theta i} B_\phi + v_{\phi i} B_\theta}_{\Delta E_r}$$



- $(V_E - V_{dim})/V_E > 60\%$  in L-mode & early I-phase but  $< 10\%$  prior to I-H transition.
- Evolutions of  $\partial V_{dim}/\partial t$  and  $V_E$  or  $V_{dim}$  are strongly correlated.
- No evident correlations between  $\partial R_s/\partial r$  and  $V_E$  are observed.



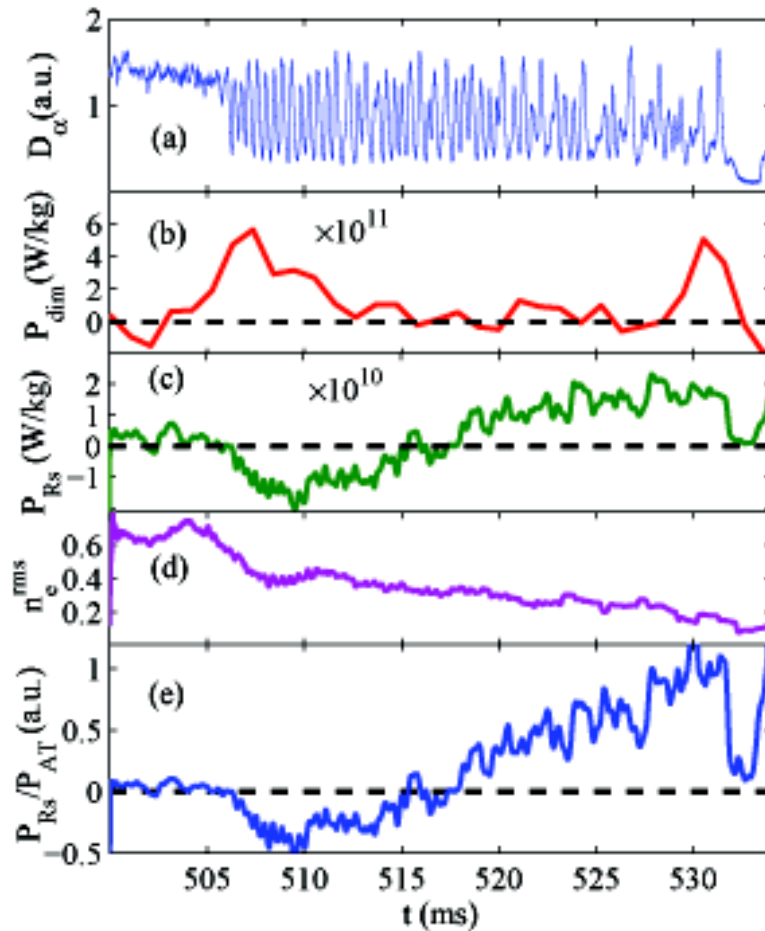
# Formation of density ETB



- The evolutions of (a)  $I_s \sim n_e$ , (b)  $\Gamma$ , (c) the phase relations between  $\Gamma$  and  $1/L_{pe}$  in LCO.
- The density increases/decreases at  $\Delta r = -6$  mm /  $-3$  mm
- The turbulent particle flux is negative/positive at  $\Delta r = -6$  mm /  $-3$  mm
- The  $1/L_{pe}$  at  $\Delta r = -6$  mm is in/out of phase with the particle flux  $\Gamma$  at  $\Delta r = -6$  mm /  $-3$  mm
- The diffusion in this region is dominated by pressure gradient induced turbulence which leads to inward particle pinch in the process of particle ETB formation.



# Rates of energy production

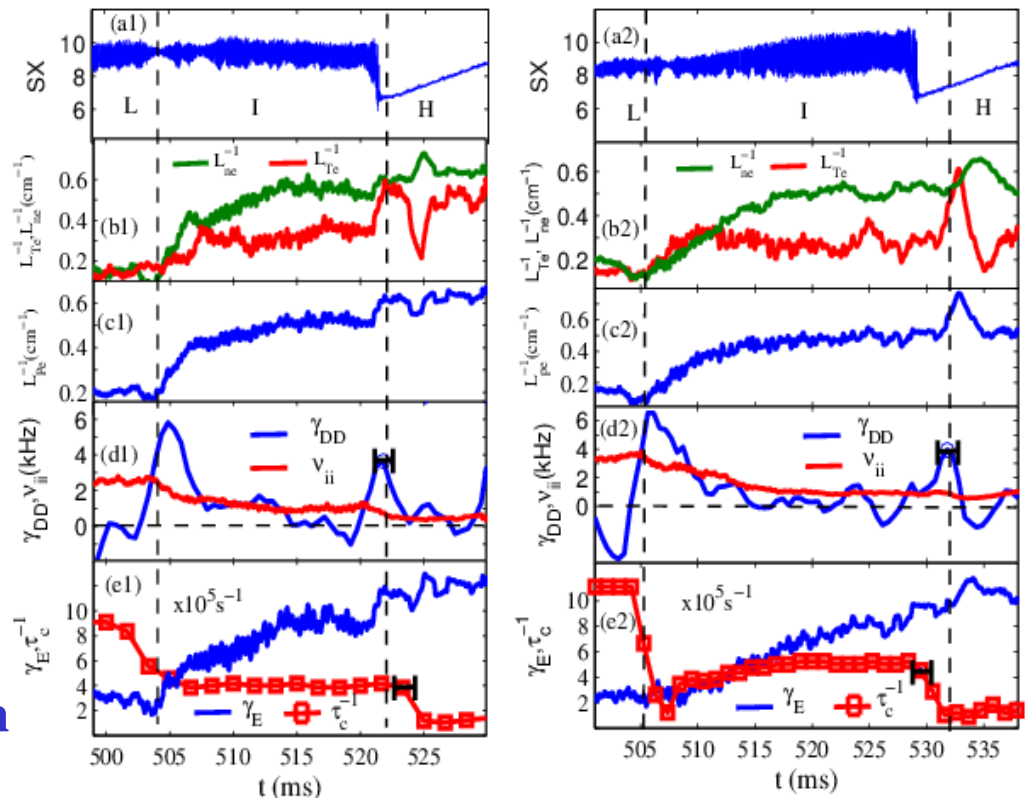


- The temporal evolutions of (a)  $D_\alpha$  emission, the flow energy production rates from (b) pressure gradient  $P_{\text{dim}}$  and (c) Reynolds stress  $P_{\text{RS}}$ , (d) RMS of the density fluctuations  $n_e^{\text{rms}}$ , (e) the ratio of  $P_{\text{RS}}/P_{\text{AT}}$ ,
- $P_{\text{dim}}$  fast increases twice prior to the L-I and I-H transitions while  $P_{\text{RS}}$  does not .
- $P_{\text{RS}}$  is negative/positive in early/late I-phase.
- $N_e^{\text{rms}}$  increases/decreases in L-mode/I-phase.
- The ratio of  $P_{\text{RS}}/P_{\text{AT}}$  has a peak prior to the I-H transition.



# Conditions for I-H transition

The time evolutions of (a) soft X-ray, (b) inverses of the scale lengths of electron temperature and density, and (c) pressure, (d) the ion-ion collision frequency and the growth rate of the diamagnetic drift flow, (e) the  $E \times B$  flow shearing rate and the turbulence decorrelation rate.



## The conditions for I-H transition

- (1) the I-phase has type-J LCOs,
- (2) the plasma pressure gradient scale length is less than a critical value ( $\sim 1.7$  cm)
- (3) the growth rate of the diamagnetic drift flow is equal to or slightly higher than the ion-ion collision frequency,
- (4) the  $E \times B$  flow shearing rate is higher than a critical value ( $\sim 10^6$  / s) and the turbulence decorrelation rate ( $4 \times 10^5$  / s).



# 4. Summary

- Two types of LCOs were observed in L-I-H transitions.
- Three plausible loops of zonal flow vs. turbulence and turbulence vs. pressure gradient are proposed for the LCOs and I-H transition.
- The dominant roles played by the diamagnetic drift flow in I-phase and I-H transition are demonstrated.
- The formation process of density ETB reveals that inward particle pinch is responsible for the barrier formation.
- The rates of energy production from diamagnetic drift and turbulent Reynolds stress for  $E \times B$  flow in L-I-H transitions are compared.
- The triggering mechanism and conditions for I-H transition are discussed.
- Much more theoretical and experimental investigations are in progress.

*Thank you  
for your attention!*

